Role of Sink Density in Nonequilibrium Chemical Redistribution in Alloys

Enrique Martínez, Oriane Senninger, Alfredo Caro, Frédéric Soisson, Maylise Nastar, and Blas P. Uberuaga

Phys. Rev. Lett. **120**, 106101 — Published 8 March 2018

DOI: 10.1103/PhysRevLett.120.106101

Role of the Sink Density in Non-Equilibrium Chemical Redistribution in Alloys

Enrique Martínez,[1,*] Oriane Senninger,[2] Alfredo Caro,[1] Frédéric Soisson,[2] Maylise Nastar,[2] and Blas P. Uberuaga[1]

[1] *Material Science and Technology Division, MST-8, Los Alamos National Laboratory, Los Alamos, 87545 NM, USA*

[2] *CEA, DEN, Service de Recherches de Métallurgie Physique, F-91191 Gif-sur-Yvette, France*

(Dated: December 13, 2017)

Non-equilibrium chemical redistribution in open systems submitted to external forces, such as particle irradiation, leads to changes in the structural properties of the material, potentially driving the system to failure. Such redistribution is controlled by the complex interplay between the production of point defects, atomic transport rates and the sink character of the microstructure. In this work, we analyze such an interplay by means of a kinetic Monte Carlo (KMC) framework with an underlying atomistic model for the Fe-Cr model alloy to study the effect of ideal defect sinks on Cr concentration profiles, with a particular focus on the role of interface density. We observe that the amount of segregation decreases linearly with decreasing interface spacing. Within the framework of the thermodynamics of irreversible processes, a general analytical model is derived and assessed against the KMC simulations to elucidate the structure-property relationship of this system. Interestingly, in the kinetic regime where elimination of point defects at sinks is dominant over bulk recombination, the solute segregation does not directly depend on the dose rate but only on the density of sinks. This model provides new insight into the design of microstructures that mitigate chemical redistribution and improve radiation tolerance.

The microstructural evolution of open systems driven far from equilibrium by the massive generation of crystalline defects depends, not only on the characteristics of the external force generating such defects and the kinetic processes controlling the migration and elimination of point defects, but also on the microstructural features that act as point defect sinks. This evolution generates mass transport within the material, inducing chemical redistribution that may lead the system to failure. Therefore, a physical model capable of predicting the steady state of a driven system resulting from the interplay between sink density, the kinetics of point defects, and the spatial redistribution of chemical species is paramount to predicting and controlling material properties.

The role of interfaces in materials under irradiation has been extensively studied in the search for radiation tolerant materials, motivated by the fact that interfaces are known to be sinks for the irradiation-created defects.[1–4] This sink behavior induces net defect fluxes in the material. In alloys, these defect fluxes couple with the alloying elements in complicated and competing ways leading to a redistribution of the chemistry, which, in general, is uncontrolled and may drive the system to unforeseen failure. This chemical redistribution is usually termed as radiation-induced segregation (RIS), which, as one example, might lead to stress corrosion cracking[5,6] as it favors the modification of the passive oxide layer promoting cracking and ultimately the breakdown of the material. Irradiation-assisted stress corrosion cracking (IASCC) and irradiation-accelerated corrosion are major concerns as material failure mechanisms for current and future nuclear reactor components.[5,6]

Ferritic/martensitic steels are foreseen as one of the main structural components in next generation fission and fusion reactors. The amount of Cr in these alloys usually ranges from 5 to 12 at.%, providing increased stability and preventing stress corrosion cracking. At the temperatures of interest and in this concentration range, Cr forms a solid solution with the Fe matrix according to the alloy equilibrium phase diagram. Nevertheless, recent experiments[7,8] show RIS and radiation-induced precipitation (RIP) in ferritic FeCr alloys. Moreover, recent experimental observations show an effect of the sink density on the RIS profiles, although they failed to provide a fundamental understanding of the observation.[9,10] Accordingly, understanding the role of irradiation in the generation of segregation profiles in these materials is of importance to assess their ability to withstand the extreme environments encountered in nuclear energy systems.

We have recently developed a lattice kinetic Monte Carlo (KMC)[11–14] model that incorporates physically accurate thermodynamic driving forces and kinetic coefficients.[15–18] The atomic interactions are based on *ab-initio* calculations for both the minimum and saddle point configurations for defect migration. Entropic effects are also considered, leading to a model that faithfully reproduces the complex phase diagram and the tracer and interdiffusion coefficients for the Fe-Cr system.[16–18] This model has proven successful for studying precipitation kinetics and reproducing the dependence of Cr concentration profiles under irradiation as compared to systematic experimental studies available in the literature.[19]

The present study focuses on the effect of interface density, modeled as planar ideal sinks, on Cr segregation profiles in Fe, and how manipulating the microstructure of the material at the nanoscale affords one route for mitigating RIS. Frenkel pairs are generated selecting a lattice site at random, removing the atom (creating a vacancy) and placing it into a second random position (creating an interstitial atom) at a prescribed dose rate. We

have modeled ideal sinks as planar regions that maintain equilibrium defect concentrations, which were taken as zero since they are orders of magnitude smaller than the irradiation-induced concentrations at the temperatures of interest. Since the very presence of sinks, inducing fluxes of defects and alloying elements, is actually the cause for RIS and RIP, is not clear *a priori* what effect the sink density has on the segregation profiles. In fact, studies of void swelling show a non-monotonic dependence of swelling with grain boundary density, with intermediate grain sizes exhibiting the greatest swelling.[20] To understand the role of interfacial density on RIS, we have run KMC simulations of Cr redistribution under various conditions of temperature, Cr content, and interfacial spacing. All simulations were run until steady-state was reached.[21] Furthermore, to rationalize our results and to provide relationships that connect interfacial density with the net amount of segregation that will prove valuable in the design of future microstructures, we develop analytical expressions starting from an atomic scale description of solute and point defect transport and based on the thermodynamics of irreversible processes.

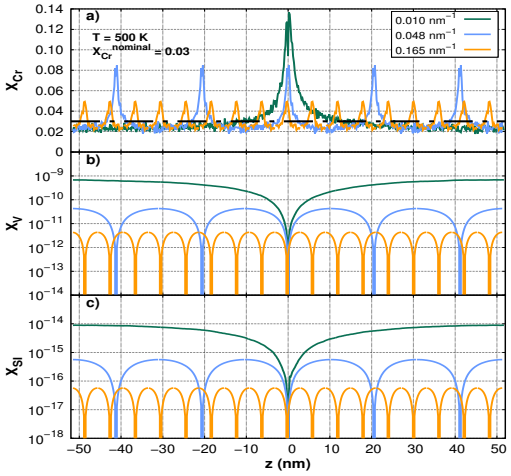

FIG. 1: (a) Cr, (b) Vacancy, and (c) Self-interstitial concentration (X) profiles at steady-state in a Fe-Cr alloy with $X_{Cr}^{nominal} = 0.03$ and at 500 K with a dose rate of 10^{-6} dpa/s for three different interface densities (0.010, 0.048 and 0.165 nm^{-1}). Results for interface densities of 0.048 and 0.165 nm^{-1} have been replicated from smaller simulation cells for clarity (in all simulations, there was only one interface in the simulation cell).

Figure 1 shows an example of the Cr, vacancy and self-interstitial steady-state concentration profiles that we obtain for a sample at 500 K with an initial homogeneous Cr concentration of $X_{Cr}^{nominal} = 0.03$ as a function of the interface density. We observe that the amount of Cr segregated at the interface decreases substantially when the sink density is increased. Both the average and the maximum concentration of defects also decrease with sink density. This suggests that increasing the interfacial density leads to a direct decrease in RIS. To quantify the relationship between Cr segregation and interface spacing, we have systematically studied the segregation profiles of Cr for a set of temperatures, nominal Cr concentrations and interface densities using our KMC model. We have measured the total amount of Cr segregated towards the sink as

$$S^{Cr} = \sum_{i}^{N_p/2} l_z \left(X_i - X_0\right) \approx \int_0^{h/2} \left(X_{Cr}(z) - X_{Cr}(0)\right) dz$$
$$= \frac{h}{2} X_{Cr}^{nominal} - \frac{h}{2} X_{Cr}(0) \quad (1)$$

where N_p is the number of atomic planes between consecutive interfaces parallel to the sink, l_z is the interplanar distance in the direction perpendicular to the interface,[22] X_i is the Cr concentration at each plane i parallel to the sink, and X_0 is the concentration farthest from the interface (center of the grain). h is the interface spacing and, assuming symmetry, we extend the integral between 0 and $h/2$ where the interface is located. The net segregation, as determined from the KMC simulations, as a function of nominal Cr concentration, interfacial spacing, and temperature is summarized in Fig. 2. We observe that the KMC data is remarkably well fit by linear functions, implying that the larger the grain size the higher the segregation. S^{Cr} can be positive or negative for enrichment or depletion, respectively. We also note that for small interface spacing (large sink densities) the total segregation tends to zero. Furthermore,

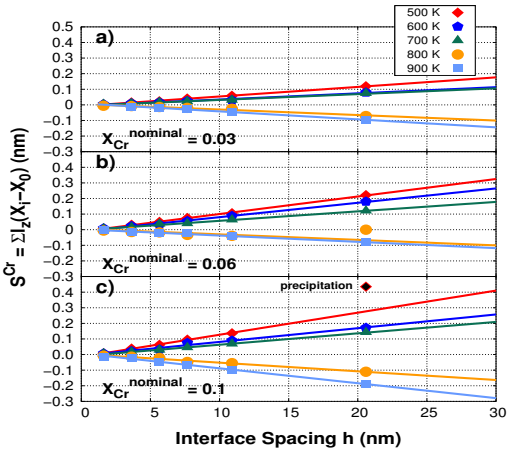

FIG. 2: Total Cr segregation S^{Cr} at steady-state as obtained by KMC simulations. l_z is the interplanar distance in the direction perpendicular to the interface, X_0 represents the Cr concentration at $z = 0$ (the farthest from the interface). The nominal Cr concentration ranges from 0.03 to 0.1 and the temperature from 500 K to 900 K. Lines represent linear fits to the data. The black dot represents simulations where precipitation occurs.

the larger the nominal concentration the higher the segregation. In this regime, when the nominal Cr concentration is close to the solubility limit, RIS can lead to precipitation of second phase particles (α' phase). These α' particles modify the material properties, leading to undesired hardening and embrittlement. Our KMC results reveal that an increased interface density not only mitigates RIS, but also the formation of α' precipitates as it prevents the local Cr concentration from reaching the solubility limit, thus suppressing RIP. Figure 3 shows an example of how RIP can be hindered by increasing the interface density. At 500 K and $X_{Cr}^{nominal} = 0.1$, precipitates are formed near the interface at an interface density $\rho^I = 0.048$ nm^{-1} (Figs. 3(a) and 3(b)). However, when the interface density is increased to $\rho^I = 0.124$ nm^{-1}, the predicted steady-state does not show α' particles in the system (Figs. 3(c) and 3(d)).

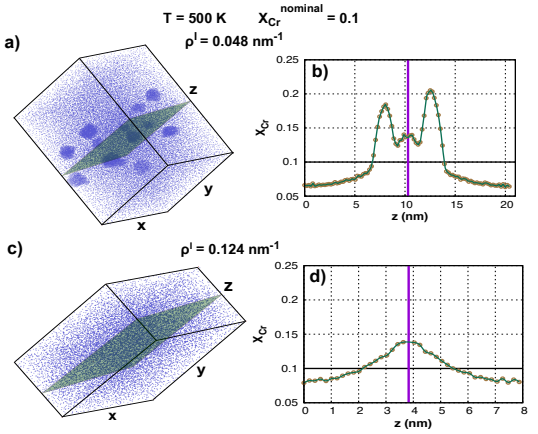

FIG. 3: KMC simulation results after an irradiation process at 10^{-6} dpa/s, 500 K and $X_{Cr}^{nominal}$=0.1 with (a)-(b) an interface density of $\rho^I = 0.048$ nm^{-1}; and (c)-(d) $\rho^I = 0.124$ nm^{-1}. The purple lines in (b) and (d) highlight the location of the interface.

In summary, our KMC simulations show that controlling the interface density is a promising approach for reducing both RIS and RIP. These findings, coupled to the known ability of interfaces to reduce the accumulation of irradiation-created defects,[1] lead to an encouraging scenario to design materials with improved radiation tolerance.

To gain a fundamental understanding of the structure-property relationship between RIS and interface density that may lead to improved material designs, we follow the development of Wiedersich *et al.*[23] to analyze the coupling between the defect fluxes and the Cr distribution. The reason is two-fold: first, to asses the validity of the expressions given by Wiedersich and, second, to obtain simple relations between the defect concentration and the Cr segregation profiles, which may aid in the design of optimal microstructures.

In the context of the thermodynamics of irreversible processes, the fluxes are given as linear combinations of thermodynamic driving forces, *i.e.*, chemical potential gradients, $J_A = -\sum_B L_{AB}\mathbb{X}_B$, with $\mathbb{X}_B = \nabla\mu_B/k_BT$, where A and B are chemical species (including defects), L_{AB} the Onsager coefficients,[24] μ_B the chemical potential of species B, k_B the Boltzmann factor and T the temperature. Following the Wiedersich formalism, at steady state, for the case where phase transitions do not occur, the gradient of the Cr and vacancy profiles near an ideal sink are related by

$$\nabla X_{Cr}(z) = \alpha(z)\frac{\nabla X_V(z)}{X_V(z)},$$
$$\text{with } \alpha(z) = -\frac{L_{FeI}L_{FeV}}{(L_{FeI}D_{Cr} + L_{CrI}D_{Fe})}\left(\frac{L_{CrV}}{L_{FeV}} - \frac{L_{CrI}}{L_{FeI}}\right), \quad (2)$$

where z is the coordinate along the direction normal to the interface, X represents element and defect concentrations, and D_A are the intrinsic diffusion coefficients, $D_A = (d^c_{AV}X_V + d^c_{AI}X_I)\Phi$ with

$$d^c_{A\delta} = \frac{L^\delta_{AA}}{X_A X_\delta} - \frac{L^\delta_{AB}}{X_B X_\delta} + d_{A\delta}\frac{1}{\Phi}\zeta_{\delta A},$$
$$A, B = \{\text{Fe}, \text{Cr}\} \text{ and } \delta = \{\text{V}, \text{SI}\} \quad (3)$$

$d^c_{A\delta}$ and $d_{A\delta}$ denote the c-partial and partial diffusion coefficients, Φ is the thermodynamic factor $\left(\frac{\nabla\mu_A}{k_BT} = \frac{\Phi}{X_A}\nabla X_A\right)$ and $\zeta_{\delta A} = \frac{\partial \ln X^{eq}_\delta}{\partial \ln X_A}$ represents an extra driving force due to irradiation.[25]

$\alpha(z)$ is a coupling factor relating the profile of chromium with that of vacancies. In general, $\alpha(z)$ depends on distance to the interface since it is a function of the phenomenological (L_{AB}) and intrinsic diffusion coefficients that, in turn, depend on local concentrations and binding energies between solutes and defects, which both vary spatially as a function of distance from the interface, as shown in Fig. 1. Also note that α can be positive or negative, depending on the sign of the term $\left(\frac{L_{CrV}}{L_{FeV}} - \frac{L_{CrI}}{L_{FeI}}\right)$, which will determine whether the sink depletes or enriches in the alloying element.

We study first the vacancy concentration profile as its main features (absolute value and gradient of the local concentration) are involved in determining the Cr concentration profile (Eq. 2). The vacancy concentration profile in the kinetic regime is obtained from the diffusion equation $D_V\frac{\partial^2 X_V}{\partial z^2} = -G$, where the recombination term and the variation of D_V with the solute composition are neglected.[26] D_V is the vacancy diffusion coefficient and G is a source term for damage production. The solution is given by $X_V(z) = -\frac{G}{2D_V}z^2 + az + b$. With the interface at $h/2$, we have the boundary conditions $\frac{\partial X_V}{\partial z}(0) = 0$, for a zero flux at $z = 0$ (the center of the grain which, by symmetry, must have zero flux) and $X_V(h/2) = X_V^{eq}$ at the interface. The solution for $0 < z < h/2$ is given by

$$X_V(z) = -\frac{G}{2D_V}(z^2 - \frac{1}{4\rho_I^2}) + X_V^{eq}, \quad (4)$$

with $\rho_I = 1/h$ the interface density. The gradient of X_V is then given by $\nabla X_V = -\frac{G}{D_V} z$. Therefore

$$\frac{\nabla X_V}{X_V} = \frac{2z}{(z^2 - \frac{1}{4\rho_I^2} - \frac{2D_V X_V^{eq}}{G})}. \quad (5)$$

Figure 4 shows the KMC results for X_V and $\frac{\nabla X_V}{X_V}$ compared to the analytical solutions of Eqs. 4 and 5. Despite the slight deviation in X_V due to the recombination term, neglected in Eq. 4 but present in the KMC results, the agreement for the $\frac{\nabla X_V}{X_V}$ term is remarkable. Note that in the KMC simulations X_V^{eq} is assumed to be zero since the concentration of vacancies due to irradiation is often significantly larger than at equilibrium. This implies that the term $\frac{\nabla X_V}{X_V}$ is independent of temperature, as obtained from the simulations.

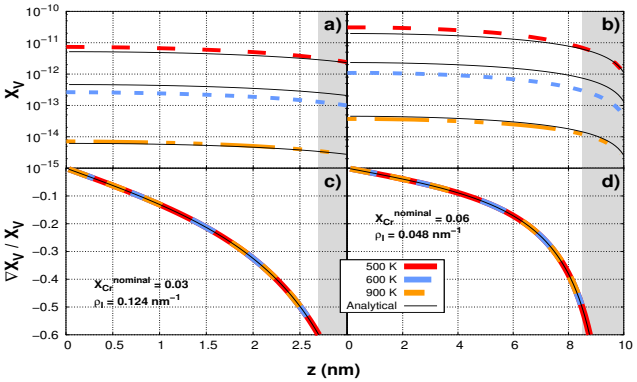

FIG. 4: (a)-(b) X_V and (c)-(d) $\frac{\nabla X_V}{X_V}$ as obtained from KMC simulations for different temperatures where no second phase precipitation occurs, compared to analytical results for (a)-(c) X_{Cr}=0.03 and a density of interfaces ρ_I=0.124 nm^{-1} and (b)-(d) X_{Cr}=0.06 and a density of interfaces ρ_I=0.048 nm^{-1}. Shaded regions represent the location of the interface. The solid black lines indicate the results of the analytical model as derived in Eqs. 4 and 5.

We now move on to the factor $\alpha(z)$ in Eq. 2. Considering the simplified case of constant α, i.e., the transport coefficients are effectively independent of local composition, we can derive an expression for the Cr concentration profile by integrating Eq. 2:

$$X_{Cr}(z) = \alpha \ln\left\{-\frac{G}{2D_V}\left(z^2 - \frac{1}{4\rho_I^2}\right) + X_V^{eq}\right\} + K_1, \quad (6)$$

with K_1 an integration constant. To determine the value of K_1 we impose mass conservation such that

$$\int_0^{h/2} X_{Cr}(z)dz = X_{Cr}^{nominal}\frac{h}{2}. \quad (7)$$

After some algebra we obtain[22]

$$S^{Cr} = -\alpha h + \alpha\frac{h}{2}\ln\left(\frac{X_V^{eq}}{a\frac{h^2}{4} + X_V^{eq}}\right) + 2b\alpha\,\mathrm{arctanh}\left(\frac{h/2}{b}\right), \quad (8)$$

with $b^2 = \frac{h^2}{4} + \frac{X_V^{eq}}{a}$ and $a = \frac{G}{2D_V}$. In the limit $X_V^{eq} \to 0$ we can write

$$\lim_{X_V^{eq}\to 0} S^{Cr} = \alpha h\,(\ln 2 - 1)\,, \quad (9)$$

which gives a simple analytical expression for the total amount of alloying element segregated to the ideal sink.[22] Equation 9 is the main result of this paper, which highlights the existence of a linear relation between S^{Cr} and the interface spacing h, with no dependence on dose rate or any other parameter not included in α. It is important to note that the behavior of the total amount of defect (vacancy and interstitial) segregation is remarkably different. Following the same methodology we obtain a cubic and a linear dependence on the interface density and the production rate G, respectively.[22] Furthermore, the linear relation for S^{Cr} with grain size derived in this work contrast with, for example, the swelling behavior, where a maximum of swelling at intermediate grain size is observed experimentally.[20] It is also important to highlight that at high temperature or for non-ideal sinks, X_V^{eq} cannot be neglected and the linear relation breaks down, although Eq. 8 will still hold.

Note that α can be obtained from the linear relations found in Fig. 2 for each temperature and Cr concentration by fitting the slope of the lines. Figure 5 shows the results for two cases. We find that Eq. 6 indeed reproduces the KMC results. Alternatively, we can also calculate α directly, following Eq. 2. We have pursued this route for the case at 600 K with $X_{Cr}^{nominal}$=0.06, and an interface density of ρ_I=0.124 nm^{-1}. We have followed the methodology described in Ref. 18 to obtain the transport coefficients, equilibrium concentrations and thermodynamic factors. The calculated value results in α=-0.028 compared to α=-0.030 obtained from fitting to the KMC. The predicted sign of the segregation profile is the same, and thus, both methods will predict enrichment near the interface. Therefore, the α obtained following either approach can be used to predict the whole Cr concentration profile via Eq. 6 at the given temperature.

It is worth mentioning that, in the same kinetic regime, the dose rate affects primarily the time to reach steady-state and not the profiles at steady-state.[22] Also, we note that in the context of collision cascade damage an effect of the production bias might be present. How production bias affects RIS profiles would be material specific since it depends on the nature and properties of the created defects and their coupling with the alloying elements. The development of an analytical expression for RIS under these conditions is far from trivial and certainly deserves a dedicated study. However, as long as the elimination of defects at interface sinks dominates over bulk recombination and the effect of production bias remains negligible,

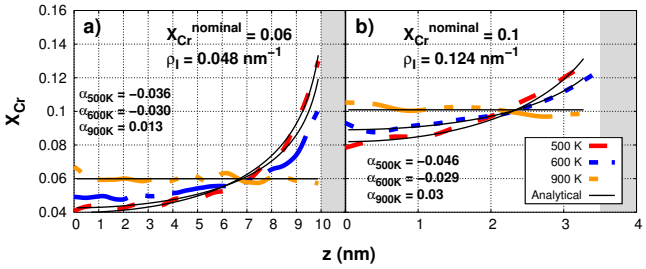

FIG. 5: X_{Cr} as obtained from KMC simulations for different temperatures at a nominal Cr composition of 0.06 and 0.1 where no precipitation occurs. Black solid lines represent analytical results from Eq. 6. Shaded regions represent the location of the interfaces.

we do not expect significant qualitative differences in the context of collision cascades beyond some correlated recombination between vacancies and self-interstitials.

In conclusion, the methodology described in this paper is a possible avenue to predict the effects of irradiation on chemical redistribution in nuclear materials. A lattice kinetic Monte Carlo model has been used to analyze the effect of the interface density on the segregation profiles in a binary alloy. We obtain linear relations between the total amount of segregation to the boundary with the interface spacing. Relying on the theory of the thermodynamic of irreversible processes, we have developed analytical expressions that indeed predict the KMC results and rationalize the effect of interface spacing on segregation. Although applied to the FeCr system, the analytical expressions derived in this work should be generally applicable to other multicomponent systems, once the material-specific transport coefficients are determined. In the kinetic regime, where elimination of point defects at sinks dominates over bulk recombination (as is typical for in-reactor conditions), the present RIS model will be able to predict the quasi-stationary RIS profile. Furthermore, given that interfaces have been shown to enhance defect annihilation and mitigate other types of radiation-induced damage phenomena, such as void swelling,[2] these results indicate that a possible venue to concurrently mitigate both damage phenomena is to control the density of high-sink-strength interfaces.

The authors are grateful for discussions with M.J. Demkowicz and A. Misra. The authors gratefully acknowledge the support of the US Department of Energy (DOE) through the LANL/LDRD Program for this work. E.M. thanks the U.S. Department of Energy, Office of Nuclear Energy, Nuclear Energy Advanced Modeling and Simulation (NEAMS) program which partially funded the theoretical developments. This research used resources provided by the LANL Institutional Computing Program. LANL, an affirmative action/equal opportunity employer, is operated by Los Alamos National Security, LLC, for the National Nuclear Security Administration of the U.S. DOE under contract DE-AC52-06NA25396.

* enriquem@lanl.gov

[1] I. Beyerlein, A. Caro, M. Demkowicz, N. Mara, A. Misra, B. Uberuaga, Radiation damage tolerant nanomaterials, Materials Today 16 (2013) 443–449.
[2] W. Z. Han, M. J. Demkowicz, N. A. Mara, E. G. Fu, S. Sinha, A. D. Rollet, Y. Q. Wang, J. S. Carpenter, I. J. Beyerlein, A. Misra, Design of radiation tolerant materials via interface engineering, Adv. Mat. 25 (2013) 6975–6979.
[3] E. Martinez, B. P. Uberuaga, I. J. Beyerlein, Interaction of small, mobile stacking fault tetrahedra with free surfaces, dislocations and interfaces in cu and cu-nb, Phys. Rev. B 93 (2016) 054105.
[4] I. Beyerlein, M. Demkowicz, A. Misra, B. Uberuaga, Defect-interface interactions, Prog. Mat. Sci. 74 (2015) 125-210.
[5] S. J. Zinkle, G. S. Was, Materials challenges in nuclear energy, Acta Mater. 61 (2013) 735–758.
[6] G. S. Was, P. L. Andresen, Stress corrosion cracking behavior of alloys in aggressive nuclear reactor core environments, Corrosion 63 (2007) 19–45.
[7] R. Hu, G. D. Smith, E. A. Marquis, Effect of grain boundary orientation on radiation-induced segregation in a Fe15.2at.% Cr alloy, Acta Materialia 61 (9) (2013) 3490–3498.
[8] J. P. Wharry, G. S. Was, A systematic study of radiation-induced segregation in ferritic-martensitic alloys, Journal of Nuclear Materials 442 (1-3) (2013) 7–16.
[9] A. Etienne, B. Radiguet, N.J. Cunningham, G.R. Odette, R. Valiev, P. Pareige, Comparison of radiation-induced segregation in ultrafine-grained and conventional 316 austenitic stainless steels, Ultramicroscopy 111 (2011) 659-663.
[10] C. Sun, S. Zheng et al., Superior radiation-resistant nanoengineered austenitic 304L stainless steel for applications in extreme radiation environments, Scientific Reports 5:7801, DOI: 10.1038/srep07801.
[11] A. B. Bortz, M. H. Kalos, J. L. Lebowitz, A new algorithm for monte carlo simulation of ising spin systems, J. Com. Phys. 17 (1975) 10–18.
[12] D. Gillespie, A general method for numerically simulating the stochastic time evolution of coupled chemical reactions, Journal of Computational Physics 22 (1976) 403–434.
[13] D. Gillespie, Exact stochastic simulation of coupled chemical reactions, Journal of Physical Chemistry 81 (1977) 2340–2361.
[14] M. Nastar, F. Soisson, Atomistic modeling of phase transformations: Point-defect concentrations and the time-scale problem, Phys. Rev. B 86 (2012) 220102.
[15] E. Martinez, C.-C. Fu, M. Levesque, M. Nastar, F. Soisson, Simulations of decomposition kinetics of fe-cr solid solutions during thermal aging, Solid State Phenomena 172-174 (2011) 1016–1021.

[16] E. Martínez, O. Senninger, C. Fu, F. Soisson, Decomposition kinetics of fe-cr solid solutions during thermal aging, Phys. Rev. B 86 (2012) 224109.
[17] O. Senninger, E. Martínez, F. Soisson, M. Nastar, Y. Bréchet, Atomistic simulations of the decomposition kinetics in fe–cr alloys: Influence of magnetism, Acta Mater. 73 (2014) 97–106.
[18] O. Senninger, F. Soisson, E. Martínez, M. Nastar, C. Fu, Y. Bréchet, Modeling radiation induced segregation in iron-chromium alloys, Acta Mater. 103 (2016) 1–11.
[19] J. Wharry, Z. Jiao, G. S. Was, Application of the inverse kirkendall model of radiation-induced segregation to ferritic-martensitic alloys, J. Nucl. Mater. 425 (2012) 117–124.
[20] B. N. Signh, M. Eldrup, S. J. Zinkle, and S. I. Golubov, On grain-size-dependent void swelling in pure copper irradiated with fission neutrons, Phil. Mag. A 82 (2002) 1137-1158
[21] To verify that the simulation results are at steady state we have made sure that the changes in the profiles of Cr, vacancies and self-interstitials are negligible in time.
[22] Supplemental Material
[23] H. Wiedersich, P. R. Okamoto, N. Q. Lam, A theory of radiation-induced segregation in concentrated alloys, J. Nucl. Mater. 83 (1979) 98–108.
[24] L. Onsager, Reciprocal relations in irreversible processes. i., Phys. Rev. 37 (1931) 405–426.
[25] M. Nastar and F. Soisson, Radiation-Induced Segregation, in Comprehensive Nuclear Materials, Elsevier 2012.
[26] F. A. Nichols, On the estimate of sink-absoprtion terms in reaction-rate-theory analysis of radiation damage, J. Nucl. Mater. 75 (1978) 32–41.